Computer Simulation of Nonlinear Ion-Electron Instability

R. H. Berman, D. J. Tetreault, T. H. Dupree, and T. Boutros-Ghali
Massachusetts Institute of Technology, Cambridge, Massachusetts 02139
(Received 14 December 1981)

A computer simulation of a one-dimensional electron-ion plasma is described. The results differ substantially from the predictions of the conventional theory of this system. In particular, an instability is observed whose onset occurs for electron drifts well below the threshold of the linear ion acoustic instability and which ultimately dominates the nonlinear evolution of the linear instability.

PACS numbers: 52.25.Gj, 52.35.Py, 52.35.Ra, 52.65.+z

We report numerical experiments for an ion-electron plasma that show an instability well below the threshold predicted by linear theory. We studied a simulation plasma with mass ratio $m_i/m_e = 4$ and temperature ratio $T_e/T_i = 1$ in which, initially, the average electron distribution $\{\langle f_e\rangle = (2\pi v_e^2)^{-1/2}\exp[-(v-v_d)^2/2v_e^2]\}$ drifts relative to the average ion distribution $\{\langle f_i\rangle = (2\pi v_i^2)^{-1/2} \times \exp(-v^2/2v_i^2)\}$. According to linear theory such a plasma is unstable (the ion acoustic instability for physical mass ratios) for drifts exceeding a certain threshold, $v_d = 3.924v_i$. We observed an instability for $v_d \geq 1.5v_i$. The observation of this instability, which is completely at variance with linear theory, is the principal result of this Letter. We describe several diagnostics that elucidate the nature of this instability. Finally, we point out that these results are consistent with recent theoretical predictions of the theory of clumps and holes. This agreement suggests that the results reported here may be the first observations of an important new type of plasma instability.

For our simulations we used a highly optimized one-dimensional, electrostatic code with $N_p = 102\,400$ particles per species. We treated a periodic system of length $L = 32.42\lambda_d$, where λ_d ($\equiv v_i/\omega_{pi}$) is the Debye length and ω_{pi} is the ion plasma frequency. Various diagnostics were performed which provide information about the fluctuations δf of the distribution function: $\delta f = f - \langle f\rangle$. For our spatially periodic and homogeneous system, the ensemble average $\langle\ldots\rangle$ was approximated by a spatial average. The two basic diagnostics we used were the mean square electric field and the mean square fluctuation $\langle(\delta N)^2\rangle$ of the number of particles, N (electron or ion), in a phase-space cell of size $\Delta x, \Delta v$. Here, $\delta N = N - \langle N\rangle$, where $\langle N\rangle$ is the mean number of particles in a cell. We would have preferred to measure the correlation function $\langle\delta f(1)\delta f(2)\rangle = \langle\delta f(x_1,v_1)\delta f(x_2, v_2)\rangle$ directly, for small $x_- = x_1 - x_2$ and small $v_- = v_1 - v_2$. Unfortunately, our value of $n_0\lambda_d = 3259.5$ ($n_0 = N_p/L$) was not large enough to provide adequate statistical accuracy. Our diagnostics, however, derive from the correlation function since the mean square electric field involves velocity integrals over $\langle\delta f\,\delta f\rangle$, while $\langle(\delta N)^2\rangle$ and $\langle\delta f\,\delta f\rangle$ are related through[1]

$$\langle(\delta N)^2\rangle = \langle[n_0\int_x^{x+\Delta v}dx\int_v^{v+\Delta v}dv\,\delta f(x,v)]^2\rangle = n_0^2\int_{-\Delta x}^{\Delta x}dx_-(\Delta x - |x_-|)\int_{-\Delta v}^{\Delta v}dv_-(\Delta v - |v_-|)\langle\delta f(1)\delta f(2)\rangle\,. \quad (1)$$

Since $\langle(\delta N)^2\rangle$ is a double integral of $\langle\delta f\delta f\rangle$, it is less sensitive to statistical error. The latter point is clearer when one realizes that Eq. (1) can be solved for the correlation function in terms of a fourth derivative of $\langle(\delta N)^2\rangle$.

We can write, for each species,

$$\langle\delta f(1)\delta f(2)\rangle = n_0^{-1}\delta(x_-)\delta(v_-)\langle f(1)\rangle + g_d(1,2) + g_v(1,2), \quad (2)$$

where the first term of Eq. (2) is the discrete-particle self-correlation function and $g_d(1,2)$ accounts for correlated fluctuations which shield the discrete particles. $g_v(1,2)$ represents the effects of fluctuations over and above this level. Using the first term of Eq. (2) in Eq. (1), we find that the self-correlation contribution to $\langle(\delta N)^2\rangle$ is $\langle N\rangle$—the value for randomly located discrete particles. This value is modified by the contribution from g_d; in particular, as the linear stability threshold is approached, the zeros of the dielectric function will enhance $\langle(\delta N)^2\rangle$ through the emission and absorption of weakly damped waves. We have calculated[2] this contribution to $\langle(\delta N)^2\rangle$ and have found it to be, consistently, much lower than the values of $\langle(\delta N)^2\rangle$ observed in the simulations (cf. Fig. 1). Our observations of $\langle(\delta N)^2\rangle$ are,

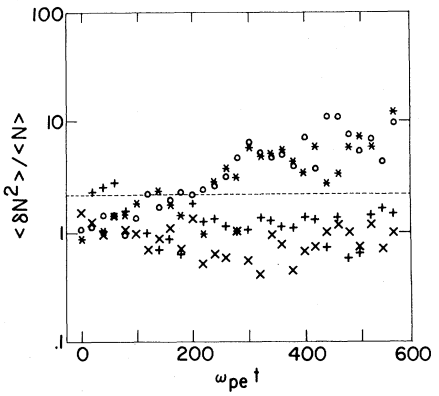

FIG. 1. Ion $\langle(\delta N)^2\rangle/\langle N\rangle$ for a phase-space cell of dimensions $\Delta x = 1.963\lambda_d$, $\Delta v = 0.1v_i$ vs time for $v_d = 2.5v_i$. The points are the simulation values measured at different velocities: crosses, $-1v_i$; plusses, $0v_i$; asterisks, v_i; and circles, $2v_i$. The dashed line is the shielded discrete-test-particle level.

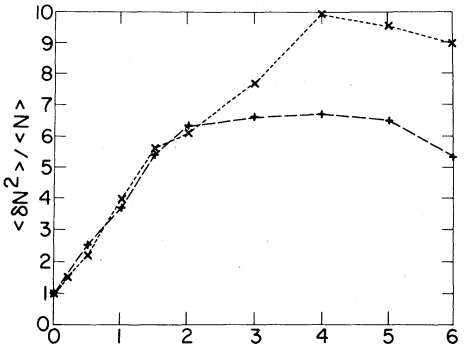

FIG. 2. Ion $\langle(\delta N)^2\rangle/\langle N\rangle$ for a phase-space cell of dimensions $\Delta x, \Delta v$. The points are the simulation values: plusses, $\langle(\delta N)^2\rangle/\langle N\rangle$ vs $20\Delta v/v_i$ at fixed $\Delta x = 0.98\lambda_d$; crosses, $\langle(\delta N)^2\rangle/\langle N\rangle$ vs $\Delta x/\lambda_d$ at fixed $\Delta v = 0.1v_i$.

therefore, evidence for collective fluctuations $g_v(1,2)$ well above the dressed test-particle level.

We measured $\langle(\delta N)^2\rangle$ in cells of size $0.05v_i \leq \Delta v \leq 3v_i$ by $0.2\lambda_d \leq \Delta x \leq 3\lambda_d$. The characteristic sizes of the fluctuations in space $(\Delta x)_c$ and in velocity $(\Delta v)_c$ were inferred from the dependence of $\langle(\delta N)^2\rangle/\langle N\rangle$ on $\Delta x, \Delta v$, given by Eq. (1). For Δx, Δv less than the characteristic size, $\langle(\delta N)^2\rangle/\langle N\rangle$ increases with $\Delta x, \Delta v$ since $\langle(\delta N)^2\rangle \simeq n_0^2\langle(\delta f^2\rangle(\Delta x \times \Delta v)^2$ and $\langle N\rangle = n_0\langle f\rangle \Delta x \Delta v$. For $\Delta x, \Delta v$ greater than the characteristic size,

$$\langle(\delta N)^2\rangle \simeq n_0^2 \Delta x \Delta v \int_{-\infty}^{\infty} dx_- \int_{-\infty}^{\infty} dv_- \langle \delta f(1)\delta f(2)\rangle$$

so that $\langle(\delta N)^2\rangle/\langle N\rangle$ approaches a constant value. For $\Delta x < (\Delta x)_c$ and $\Delta v > (\Delta v)_c$, and vice versa, $\langle(\delta N)^2\rangle$ becomes proportional to Δx and Δv, respectively. Figure 2 is a typical plot of $\langle(\delta N)^2\rangle/\langle N\rangle$, for the ions, versus cell size. It indicates that the ion fluctuation curves stopped increasing and turned over when $\Delta x \simeq 4\lambda_d$ and $\Delta v \simeq 0.1v_i$. Thus, these values of Δx and Δv represent the characteristic sizes $(\Delta v)_c$ and $(\Delta x)_c$.

Figure 1 shows the time dependence of $\langle(\delta N)^2\rangle/\langle N\rangle$ for the ions for a run with $v_d = 2.5v_i$. After starting at unity, $\langle(\delta N)^2\rangle/\langle N\rangle$ has risen by $\omega_{pe}t = 150$ to the shielded discrete-particle level, which we calculated to be 2.2. Subsequently, growth occurred until $\omega_{pe}t = 300$. Following this unstable growth phase, the instability saturated when the electron distribution function formed a plateau in velocity space. We measured the fluctuation levels at $-v_i$, 0, v_i, and $2v_i$. Fluctuations with phase velocities of v_i and $2v_i$ grew, while those at 0 and $-v_i$ decayed. This would seem to indicate that the instability grows in regions of opposing velocity gradients of $\langle f_e\rangle$ and $\langle f_i\rangle$. Furthermore, we note that the instability occurred in regions of large negative $\partial\langle f_i\rangle/\partial v \neq 0$—a region where linear theory would predict strong damping of the fluctuations. Figure 3 shows that the fluctuations are unstable over a wide region of velocity space ($0 \leq v \leq 4v_i$). This is evidenced by the ion tail and distorted electron distribution at $400\omega_{pe}^{-1}$. These distortions in $\langle f_i\rangle$ and $\langle f_e\rangle$ are not the result of discrete-particle collisions, since the collisional relaxation time is substantially larger than the run time of the simulation. Moreover, ion acoustic waves cannot be responsible, since, according to linear theory, they are stable.

Numerous runs were made to study various

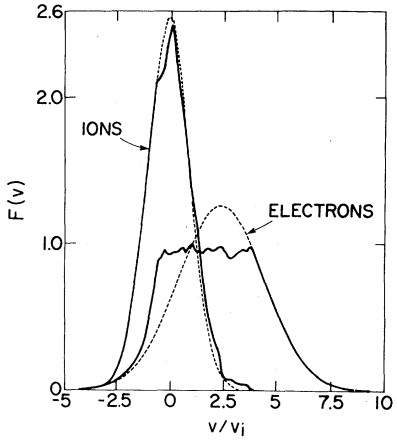

FIG. 3. The spatially averaged distribution functions for the ions and electrons for $v_d = 2.5v_i$ at $\omega_{pe}t = 400$ (solid curve) and at 0 (dashed curve).

features of the instability: First, we examined the effect of using different initial conditions to start the simulation. These included quiet starts with $\langle(\delta N)^2\rangle/\langle N\rangle \ll 1$; "thermal-level" starts with $\langle(\delta N)^2\rangle/\langle N\rangle \approx 1$; and "noisy" starts with $\langle(\delta N)^2\rangle/\langle N\rangle \approx 4$. In all cases an instability was observed for $v_d \geq 1.5v_i$. Thus, to trigger the instability we did not require large-amplitude fluctuations. In fact, the amplitude $\langle(\delta N)^2\rangle/\langle N\rangle \simeq 1$ corresponds to $e\langle\varphi^2\rangle^{1/2}/m_i v_i^2 \simeq 10^{-2}$, where $\langle\varphi^2\rangle$ is the mean square potential.

Second, we investigated the dependence of the instability on v_d. Aside from the growth rate, there were no apparent qualitative differences between the runs for $1.5v_i \leq v_d \leq 4.5v_i$. After an initial growth stage, the instability saturated by forming a quasilinear plateau. The ion distribution function developed a tail and the electron distribution function became significantly flattened as indicated in Fig. 3. We emphasize that these distortions were evident for v_d both below and above the linear stability threshold. The dependence of γ, the observed growth rate, on v_d is illustrated in Fig. 4. The measurements were made, for the ions, at approximately the same amplitude $\langle(\delta N)^2\rangle/\langle N\rangle$ for each run [the electron $\langle(\delta N)^2\rangle/\langle N\rangle$ gave similar growth rates]. The error bars indicate the spread in the measured values of the growth rate when different methods were used to obtain γ. These methods consisted of measuring γ from the mean square electrostatic field, and from the time dependence of

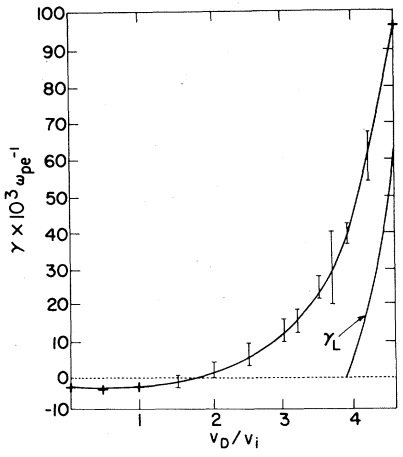

FIG. 4. The simulation values of the growth rate γ vs the electron drift v_d. Plusses denote single measurements while the error bars include several measurements. The growth rate γ_L obtained from linear stability theory is also plotted.

$\langle(\delta N)^2\rangle/\langle N\rangle$ at different phase velocities ($v/v_i = 0.5, 1, 2$), and different cell sizes ($\Delta x/\lambda_d = 1, 2$, $\Delta v/v_i = 0.1, 0.2$). Also shown in Fig. 4 is the linear growth rate γ_L for the most unstable wave number. It is clear that the nonlinear effects dominated in the linearly unstable, as well as the linearly stable, region since $\gamma_L < \gamma$.

The third feature we examined was the effect of varying the parameter $n_0\lambda_d$. When we decreased $n_0\lambda_d$ to 815, no change in γ occurred. From this, we concluded that discrete-particle collisions apparently did not play an important role. Below the nonlinear threshold, we saw the fluctuations decay. For $v_d = 0$, we measured the same decay rate observed in a series of one-species calculations with $n_0\lambda_d = 65\,190$ reported elsewhere.[3]

The measured characteristics of the instability are consistent with the nonlinear theory of ion and electron "clump" regeneration.[4] In a Vlasov plasma, clumps result from the mixing of the incompressible phase-space density by turbulent fluctuations.[5,6] If the clump production rate is equal to their destruction rate (through velocity streaming and the turbulent electric fields) the clump spectrum will regenerate. Overregeneration implies an instability. In Ref. 4 it was theoretically predicted, for the parameters of this simulation, that a clump spectrum would regenerate in regions of opposing velocity gradients for $v_d \geq 2.5v_i$. In addition, the spectrum would exhibit a wide phase-velocity spread (of the order of v_i) and characteristic scales similar to those observed in this simulation. Moreover, approximate calculations[7] show that for a mass ratio of 4, the clump instability has an amplitude-dependent growth rate proportional to the inverse ion trapping time $[\tau_{tr} \equiv (\Delta x)_c/(\Delta v)_c]$. The constant of proportionality (which is of the order of unity) increases rapidly with v_d and $-(\partial\langle f_e\rangle/\partial v)\partial\langle f_i\rangle/\partial v$. The observed values of $(\Delta x)_c$ and $(\Delta v)_c$ lead to a trapping time of the order of $80\omega_{pe}^{-1}$ which is consistent with the measured growth rates (cf. Fig. 4).

The existing calculations of clump regeneration omit a number of terms that describe the effects of self-binding of the fluctuations. Clumps are enhancements ($\delta f \geq 0$) or depletions ($\delta f \leq 0$) in the local phase-space density. The depletions, or "holes," have the property of being self-binding.[8] Such an effect would decrease the destruction rate of the fluctuations and therefore reduce the predicted drift-velocity threshold. This would also be consistent with the slow (about $0.1\tau_{tr}^{-1}$) decay rate observed at $v_d = 0$. It is interesting to note

that a single, isolated phase-space hole has been shown to be unstable for all $v_d > 0$.[9] This isolated-hole instability is driven by opposing velocity gradients of $\langle f_i \rangle$ and $\langle f_e \rangle$ and is the analog to the turbulent clump instability.

Although the nonlinear instability discussed in this Letter is one dimensional and driven by velocity gradients, we believe that it is representative of an important new class of instabilities since clump and hole phenomena are predicted to occur in three dimensions with a magnetic field. For instance, it recently has been shown that a single phase-space hole in a magnetic field is unstable to a spatial density gradient.[9] This result implies that the clump instability will be driven by a spatial density gradient. Furthermore, our simulation indicates that large amplitudes are not necessary for its onset. Indeed, we have observed the instability growing out of thermal-level fluctuations.

This work is supported by the National Science Foundation and the Department of Energy. Parts of these computations were performed using MACSYMA and LISP machines at Massachusetts Institute of Technology.

[1]T. H. Dupree, C. E. Wagner, and W. M. Manheimer, Phys. Fluids 18, 1167 (1975).

[2]The calculation is for the case $\Delta x, \Delta v, > (\Delta x)_c, (\Delta v)_c$. For smaller-size windows $\langle (\delta N)^2 \rangle$ would be smaller.

[3]R. H. Berman, D. J. Tetreault, and T. H. Dupree, Bull. Am. Phys. Soc. 25, 1035 (1980), and in Proceedings of the Ninth Conference on Numerical Simulation of Plasmas, Chicago, 1980 (to be published).

[4]T. Boutros-Ghali and T. H. Dupree, to be published.

[5]T. H. Dupree, Phys. Fluids 15, 334 (1972).

[6]T. Boutros-Ghali and T. H. Dupree, Phys. Fluids 24, 1839 (1981).

[7]D. J. Tetreault, "Growth rate of the Clump Instability" (to be published).

[8]T. H. Dupree, Phys. Fluids 25, 277 (1982).

[9]T. H. Dupree, Bull. Am. Phys. Soc. 26, 1060 (1981).

Experimental Observations of Rotamak Equilibria

G. Durance,[a] B. L. Jessup,[b] I. R. Jones, and J. Tendys [a]

School of Physical Sciences, The Flinders University of South Australia, South Australia 5042, Australia

(Received 11 February 1982)

Some experimental observations of rotamak equilibria made in a high-power, short-duration (~ 80-μs) experiment and a complementary low-power, long-duration experiment are summarized. In the high-power experiment two possible equilibrium phases have been identified: an oblate, compact torus configuration and a $\beta = 1$, mirrorlike configuration. In the low-power experiment toroidal plasma current has been driven, and a compact torus configuration has been maintained, for several milliseconds.

PACS numbers: 52.55.Gb

Compact toroid configurations are currently attracting great interest because of their potential engineering advantages compared with other toroidal fusion systems. In early 1979 the proposal[1] was made that the rotating-field method of generating plasma currents[2-5] be wedded with the compact toroid approach to fusion in an apparatus which has subsequently come to be known as the rotamak.

In the rotamak concept, a rotating magnetic field is used to drive the steady toroidal current in a compact torus device. An externally applied "vertical" field couples with this toroidal plasma current to provide the inwardly directed force necessary for the equilibrium of the plasma ring. A full description of the magnetic configuration and of the experimental device can be found in Refs. 6 and 7. In the period since the publication of Refs. 6 and 7, an extensive series of current and magnetic field measurements have been made, both on a high-power, short-duration rotamak device and on a complementary, low-power, long-duration apparatus. In neither of these experiments was a steady toroidal field employed. In this Letter we present a summary of the more important observations that have been made on rotamak equilibria in these two experiments.

The high-power, short-duration experiment differed from the one described in Refs. 6 and 7 in two respects. The frequency and duration of the rotating field were 0.35 MHz and ~ 80 μsec, respectively (cf. 0.67 MHz and ~ 16 μsec), and